Scientific research article

Cancer drug therapy by Gemcitabine derivatives with PEG linker for gynecological disease, beside speech therapy in implementation of biomedical caring of post-operative

Majid Monajjemi[1]*, Fatemeh Mollaamin[2], Azam Ghadami[3], Reyhaneh Souri[3], Zahra Aghakouchaki[3], Melika Aghaei[4], Zahra Solati[4] & Yasamin Shahverdy[4]

[1] Department of Biology, Faculty of Science, Kastamonu University, Kastamonu, Turkey.
[2] Department of Biomedical Engineering, Faculty of Engineering and Architecture, Kastamonu University, Kastamonu, Turkey.
[3] Department of Polymer Engineering, CT.C., Islamic Azad University, Tehran, Iran.
[4] Department of Chemical Engineering, CT.C., Islamic Azad University, Tehran, Iran.

Corresponding author E-mail: maj.monajjemi@iauctb.ac.ir; m_monajjemi@yahoo.com

Received: March 19, 2025
Corrected: November 11, 2025
Accepted: November 13, 2025

https://doi.org/10.15446/rcciquifa.v55n1.125080

SUMMARY

Background: Although Gemcitabine is applied for chemotherapy as an important drug for breast, head and neck, lung, bladder, as well as acute lymphocytic leukemia, non-Hodgkin's lymphoma, osteosarcoma, and choroid carcinoma, we found derivatives combination of Gemcitabine enable to increase the effectiveness for cancer treatment significantly and these derivatives drugs can be used for decreasing desmoids tumor in the treatment of aggressive fibromatosis. **Aim:** Therefore, our goal was based on analyzing of a series of gemcitabine derivatives containing imine structure (G1-G5), which can be synthesized through reaction of gemcitabine with several aromatic aldehydes for this research and any further activities such as drug design or drug delivery. **Materials and methods:** Furthermore, the structures of the imine derivatives were proved via CHNS/O elemental analysis, FTIR and NMR spectroscopy, which all measurements confirmed the imine derivatives of α-glucosidase inhibition. **Results:** Compound (G5) exhibited higher therapeutic indices, representing possible promising roles. We used gemcitabine derivatives containing Schiff base structure (G5) for patient that could be lead a new design in this study of novel α-glucosidase inhibitor. **Conclusions**: surgery disrupts the physiological balance of the human body and causes great stress and changes hormonal, metabolic, immune and nervous functions, using this drug (G5) during recovery after surgery (ERAS) is a multitasking care process that preserves the normal physiological state and reduces surgical complications of surgery.

Keywords: Gemcitabine derivatives; ERAS guidelines; rehabilitation after surgery; gynecological cancer; post- operative; biomedical caring; oncology; genome map

RESUMEN

Terapia oncológica con derivados de gemcitabina con enlace PEG para enfermedades ginecológicas, además de terapia del habla en la implementación de cuidados biomédicos postoperatorios.

Antecedentes: Si bien la gemcitabina se utiliza en quimioterapia como fármaco importante para el cáncer de mama, cabeza y cuello, pulmón, vejiga, leucemia linfoblástica aguda, linfoma no Hodgkin, osteosarcoma y carcinoma coroideo, hemos descubierto que la combinación de derivados de gemcitabina permite aumentar significativamente la eficacia del tratamiento oncológico. Estos derivados también pueden utilizarse para reducir el tumor desmoide en el tratamiento de la fibromatosis agresiva. **Objetivo:** Por lo tanto, nuestro objetivo se basó en el análisis de una serie de derivados de gemcitabina con estructura imina (G1-G5), sintetizados mediante la reacción de gemcitabina con diversos aldehídos aromáticos, para esta investigación y otras actividades como el diseño o la administración de fármacos. **Materiales y métodos:** Las estructuras de los derivados de imina se confirmaron mediante análisis elemental CHNS/O, espectroscopía FTIR y RMN, mediciones que corroboraron la inhibición de la α-glucosidasa por parte de estos derivados. **Resultados:** El compuesto (G5) mostró índices terapéuticos superiores, lo que sugiere posibles aplicaciones prometedoras. En este estudio, utilizamos derivados de gemcitabina con estructura de base de Schiff (G5) para pacientes que podrían ser candidatos para un nuevo diseño de inhibidor de la α-glucosidasa. **Conclusiones:** La cirugía altera el equilibrio fisiológico del cuerpo humano, provoca un gran estrés y cambios en las funciones hormonales, metabólicas, inmunitarias y nerviosas. El uso de este fármaco (G5) durante la recuperación posquirúrgica (ERAS) constituye un proceso de cuidados integrales que preserva el estado fisiológico normal y reduce las complicaciones quirúrgicas.

Palabras clave: Derivados de gemcitabina; protocolos ERAS; rehabilitación posquirúrgica; cáncer ginecológico; posoperatorio; cuidados biomédicos; oncología; mapeo genómico.

RESUMO

Terapia medicamentosa contra o câncer com derivados de gencitabina com ligante PEG para doenças ginecológicas, além de terapia fonoaudiológica na implementação do cuidado biomédico pós-operatório

Contexto: Embora a gencitabina seja utilizada na quimioterapia como um importante medicamento para câncer de mama, cabeça e pescoço, pulmão, bexiga, bem como leucemia linfoblástica aguda, linfoma não Hodgkin, osteossarcoma e carcinoma de coroide, descobrimos que a combinação de derivados de gencitabina permite aumentar significativamente a eficácia do tratamento do câncer e que esses derivados podem ser usados para reduzir o tumor desmoide no tratamento da fibromatose agressiva. **Objetivo:** Portanto, nosso objetivo foi analisar uma série de derivados de gencitabina contendo estrutura imina (G1-G5), que podem ser sintetizados por meio da reação da gencitabina com diversos aldeídos aromáticos, para esta pesquisa e quaisquer atividades futuras, como o planejamento ou a administração de fármacos. **Materiais e métodos:** Além disso, as estruturas dos derivados de imina foram comprovadas por meio de análise elementar CHNS/O, espectroscopia FTIR e RMN, cujas medições confirmaram a inibição da α-glicosidase pelos derivados de imina. **Resultados:** O composto (G5) apresentou índices terapêuticos mais elevados, representando possíveis aplicações promissoras. Utilizamos derivados de gencitabina contendo estrutura de base de Schiff (G5) em pacientes, o que pode levar a um novo desenvolvimento de inibidores da α-glicosidase neste estudo. **Conclusões:** A cirurgia perturba o equilíbrio fisiológico do corpo humano e causa grande estresse, além de alterar as funções hormonais, metabólicas, imunológicas e nervosas. O uso deste fármaco (G5) durante a recuperação pós-cirúrgica (ERAS) é um processo de cuidado multifuncional que preserva o estado fisiológico normal e reduz as complicações cirúrgicas.

Palavras-chave: Derivados de gencitabina; diretrizes ERAS; reabilitação pós-cirúrgica; câncer ginecológico; pós-operatório; cuidados biomédicos; oncologia; mapeamento genômico

1. INTRODUCTION

1.1. Gemcitabine & Methotrexate for chemotherapy drugs

Gemcitabine as a chemotherapy medication generally applied breast, ovarian cancer, lung cancer, and pancreatic cancer, so this drug is mostly has been used for gynecological cancer through intravenous infusion [1]. The side effects of this drug related to the bone marrow problem, liver and kidney disease, nausea, fever, rash, shortness of breath, mouth sores, diarrhea, neuropathy, and hair loss [2]. Although this drug was synthesized in 1983, was not confirmed up to 1995 [1, 2]. This drug enables to block the creation of new DNA that causes in cell death [3]. Gemcitabine operated as a first-line treatment for pancreatic cancer and also metastatic cancer such as advanced bladder through combination with cisplatin (or with Methotrexate). Moreover, enable for treatment in combination with carboplatin for ovarian cancer and in combination with paclitaxel for metastatic breast cancer instead of surgically removed [3], finally it is dangerous for women who taking gemcitabine should not become pregnant. Gemcitabine inside DNA permits a native nucleoside base to be added in the strains and mask the chain as a "faulty" base, and eludes the cell's normal repair system (base-excision repair), consequently creates an irreparable error that causes to inhibition of further DNA synthesis towards cell death [1-6] (Figure 1).

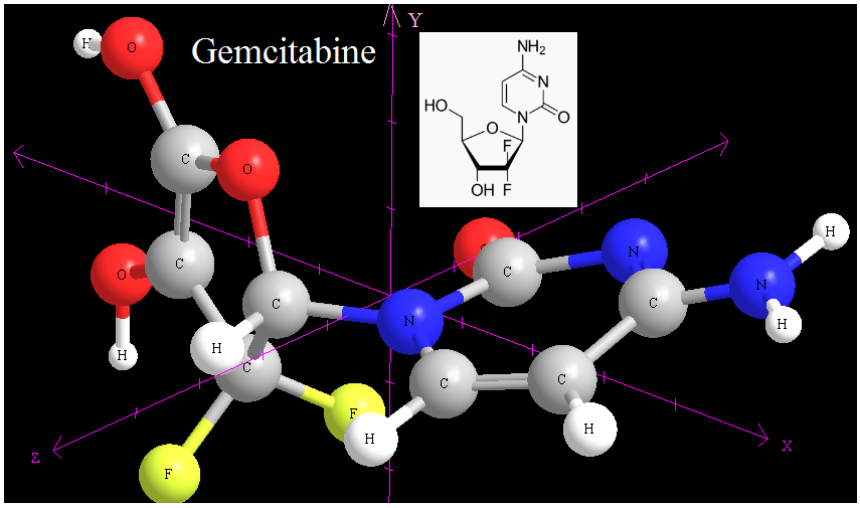

Figure 1. Gemcitabine optimized by B3LYP/6-31g* level of theory.

1.2. Biological effective of a bipill, with gemcitabine (GEM) and methotrexate (MTX)

Recent works reported the biological evaluation of a bipill, via appending two different anticancer agents, viz., gemcitabine (GEM) and methotrexate (MTX), to the distal ends of poly (ethylene glycol) (PEG) spacer. These type covalent binding between GEM and MTX through PEG linker not only transformed the solubility profiles of constituent drug molecules, but also considerably improved their stability in the presence of plasma. In vitro cytotoxicity studies confirmed that GEM-PEG-MTX treats higher cytotoxicity in gynecological cancers such as adenocarcinoma MCF-7 cell lines, when compared to free drug congeners, i.e., free GEM and free MTX. Consequently, dual drug conjugation is an effective means to synergize the therapeutic indices of potential drug candidates while alleviating drug-associated side effects [7] (Figure 2).

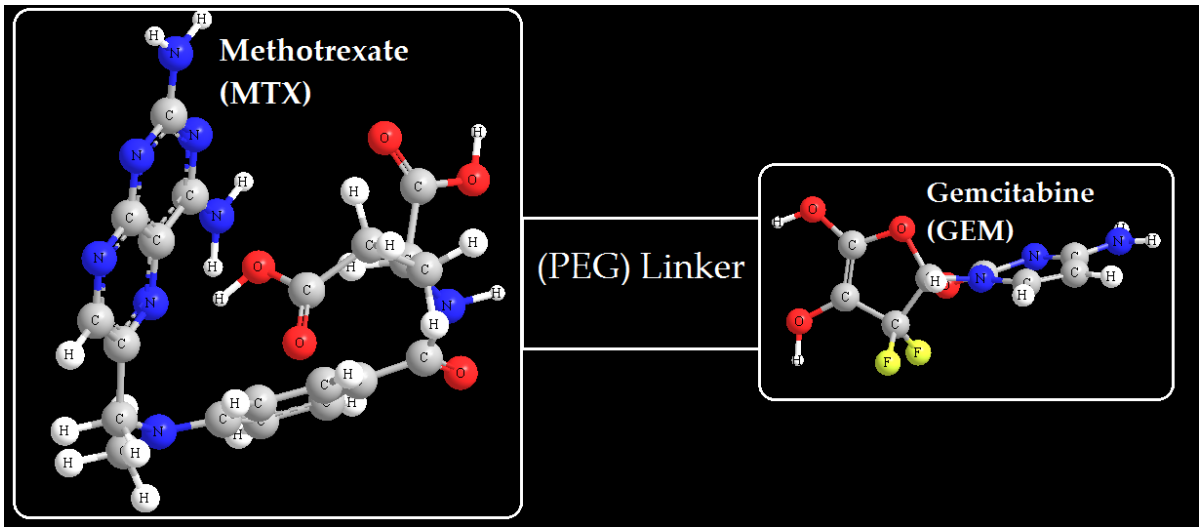

Figure 2. Biological structure of a bipill, with gemcitabine (GEM) and methotrexate (MTX).

2. BACKGROUND OF CHEMICAL SYNTHESIS AND MECHANISM

2.1. Gemcitabine synthesis

The initial synthesis of gemcitabine was done in the Lilly research laboratories, and was illustrated by Hertel *et al.* in 1988 (Figure 3). A Linear Synthesis of Gemcitabine was also accomplished by Kylie Brown *et al.* in 2015 [8]. The synthesis begins by D-glyceraldehyde that could be provided from D-mannitol in two reactions. Using ethyl bromic-di-fluoro-acetate, under standard temperature and pressure by yielded a 3:1 mixture. Gemcitabine is hydrophilic therefore inserted inside the cells through material transporters such as SLC29A1, SLC28A1, and SLC28A3. During inserting slowly linked to phosphate of DNA to produce gemcitabine monophosphate (dFdCMP and this step is a major process for definition of reaction velocity, which is catalyzed by the enzyme deoxycytidine kinase (DCK). After attaching of two other phosphates the three phosphates gemcitabine complex is produced that structurally active for reaction and known as (dFdCTP). Due to the thrice phosphorylated, this complex can masquerade as deoxycytidine triphosphate in DNA structures as new DNA strands during synthesized of the cell replicates [9].

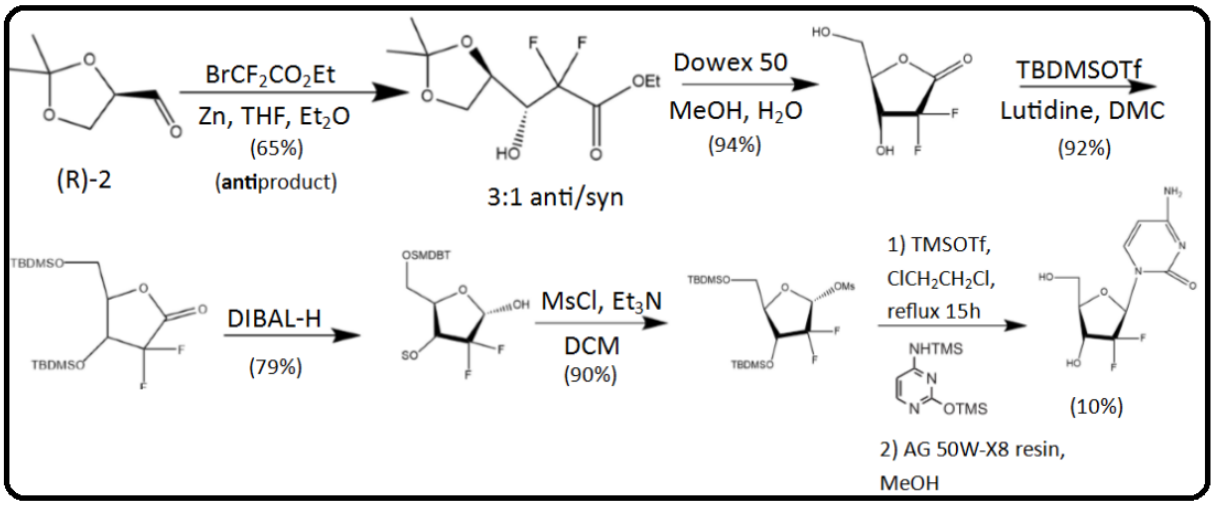

Figure 3. First synthesis of Gemcitabine process by Hertel *et al.* at Lilly laboratories in 1988.

The compound **8** has been employed as starting material in the synthesis of gemcitabine and homo-gemcitabine, also with a Reformatsky reaction as the key step (Figure 3). However, no diastereomeric ratio was given. Presumably, the re-crystals step after the actinide hydrolysis/ sequence allowed separation of the diastereomers, leading to diastereomerically pure **10**. Protection and lactone reduction then gave the difluorolactol **11**. In addition to ethyl- bromic-difluoro-acetate as fluorinated building block, 2-deoxy-2,2-difluororibose has also been synthesized using Reformatsky-type reactions with other reagents (Figure 3). Treatment of bromic-di-fluoro-acetylene **12** with zinc, followed by reaction with D-glyceraldehyde actinide (R)-2, led to the addition product **13** in 50% yield, as a 3/1 anti/syn ratio **14**. Diastereomeric separation using flash chromatography was possible, and anti-**13** was subjected to partial alkyne hydrogenation, ozonolysis /Me2S treatment, with final protection of the obtained product **14** as the triacetate **15** (Figure 4) [10, 11].

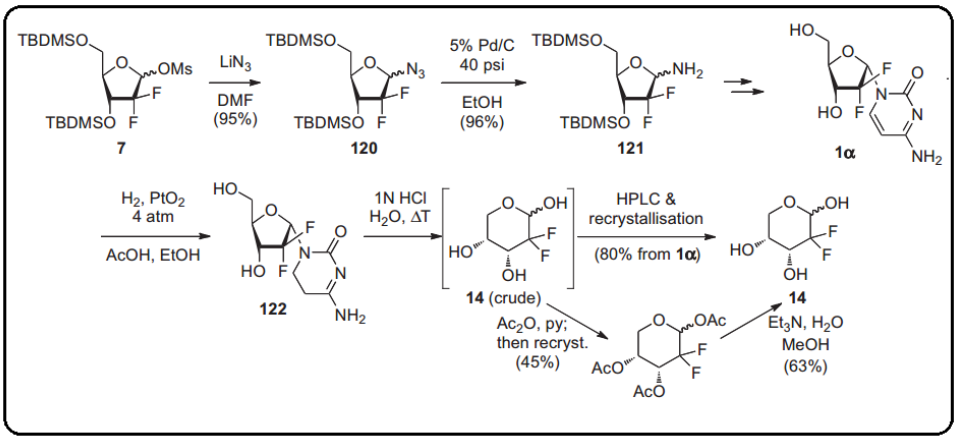

Figure 4. Reformatsky reaction on L-threose derivative and alternative Reformatsky reagents **12** and **16** in the synthesis of 2-deoxy-2,2-difluororibose.

2.2. Aldol reactions

Various systems exhibit the reaction of glycerol-de-hydro-acetate with di-fluoro-acetate from enolate type compounds (Figure 5). The lithium enolate **23** from ethyl di-fluoro-acetate **18** exhibits hampered via Claisen self-condensation side reaction. Beginning from t-butyl-difluoro-thiol-acetate **19**, reached to the formation of lithium enolate **24**, which it is structured through adding **19** to a slight excess of LDA at 80 °C, and then quickly reacted with the electrophile. It is notable the Claisen product is produced by a partial amount (10%) yet and but avoided from forming the corresponding ketene silyl O,S-acetyl **25** (Figure 5).

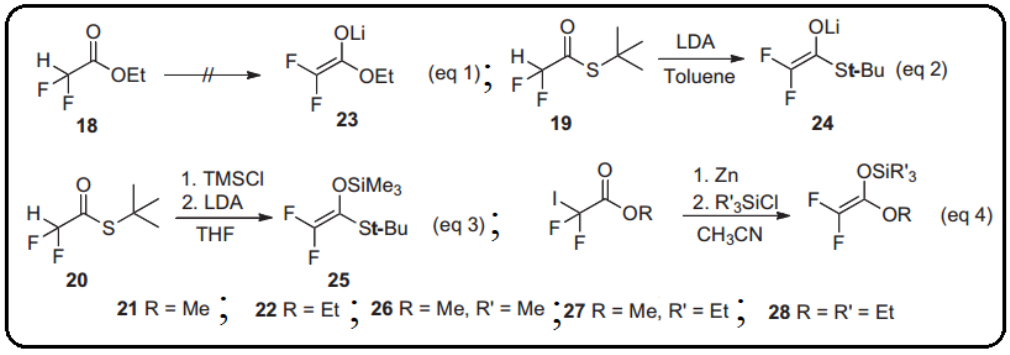

Figure 5. Synthesis of the difluoro-enolate derivatives.

Equation 4 denotes to the formation of ketene silyl acetyls **26–28** via a modification of the Reformatsky conditions, in which a tri-alkyl-chlorosilane was included in the reaction mixture before addition of the electrophile. Similar approaches were used from **22** instead of the **21** to give the silyl ketene acetyl **28**. The resulting product prepared in a lower ratio despite a cyclohexylidene acetyl protected glyceraldehyde [12]. This amount of relationship from rationalize are typically obtained with this protecting group compared to the corresponding actinide. The reactions containing **26–28** (entries are basically Mukaiyama aldol reactions, and these were reached without the addition of a Lewis-acid. *In situ* it was formed to ZnI_2, which was responsible for activating the aldehyde group. Matsumura *et al.* [13] studied on the influence of Lewis acid addition in the presence of BF_3OEt_2, similar anti/syn selectivity was obtained, but in lower yield (Figure 6).

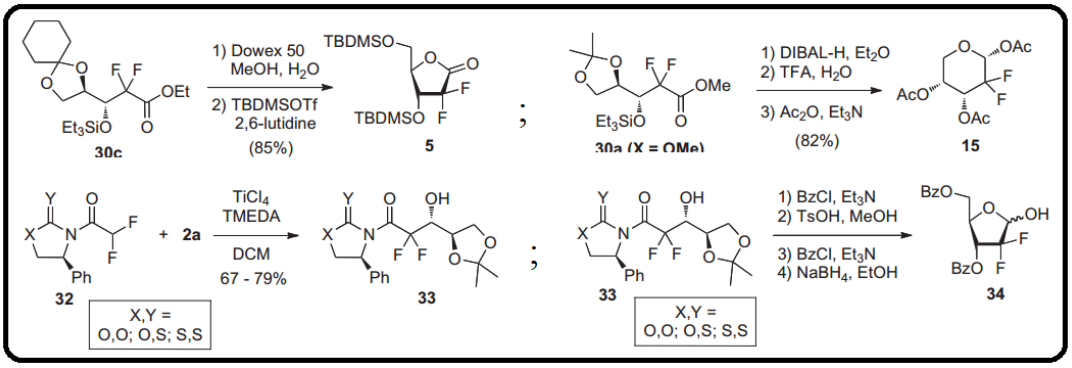

Figure 6. Homo-chiral enolate derivatives and further functional of the aldol products to di-fluoro-ribose derivatives.

3. MATERIAL AND METHODS

3.1. Imine derivatives of Gemcitabine

Configuration and designing of this work have been accomplished based on some of our previous works [14-23]. We also used Silica-Gel (From Germany known as SG-40 Merck) in thin layer chromatography (TLC) with distillated solvents. Infrared spectra were measured by ALPHA II- FT-IR spectrometer from Bruker Company. CHNS/O elemental analysis, determines the percentage of Carbon (C), Hydrogen (H), Nitrogen (N), Sulfur (S) and Oxygen (O) present in a sample, which this technique is reliable and cost-effective to assess the purity and chemical composition of compounds. These analyzing were measured by EMA 502 Elemental Analyzer CHNS-O. NMR spectrums were measured by Avance NMR Spectrometer (Bruker company) (^{1}H-NMR 500 MHz and ^{13}C-NMR 75 MHz). An amount by 0.02 moles of gemcitabine was mixed by 0.02 moles for each of several benzaldehydes including (G1): 4-methylbenzaldehyde, (G2): 4-bromobenzaldehyde, (G3): 4-chlorobenzaldehyde, (G4): *N,N*-di-methyl-benzaldehyde, and (G5): 4-hydroxybenzaldehyde, inside 40 mL C_2H_5OH. Gradually and slightly glacial acetic acid was added to the mixture and keep out at 90 °C. During monitoring the reaction (by TLC), the product was separated with 80 mL of diethyl ether. After evaporated diethyl ether the product was dried and purified (Figure 7).

3.1.1. "G1": Gemcitabine derived by 4-methylbenzaldehyde

This compound was prepared through mentioned instruction by Formula: $C_{17}H_{17}F_2N_3O_4$; during temperature around 130 °C, with purification of 80%. FTIR results indicated a 3409 cm^{-1} for OH stretching, 3119 cm^{-1} for C-H bound in aromatic position, 2939 cm^{-1} for C-H bound in

aliphatic stretching, 1669 cm^{-1} for C=O stretching, 1579 cm^{-1}, 1541 cm^{-1} for C=N and C=C, respectively. As well as proton NMR in DMSO solvent beside TMS reference, indicated the chemical shifts as follows δ = 8.51 for HC=N imine, 7.69 for HC=N pyrimidine ring, and 7.29-7.19 for Ar-H. In addition, ^{13}C-NMR at (75 MHz) exhibited δ=165.02, 149.99, 139.84, 139.21, 129.61, and 130.01 for those bonds, respectively.

3.1.2. "G2": Gemcitabine derived by 4-bromobenzaldehyde

This compound was prepared through mentioned instruction by formula $C_{16}H_{14}BrF_2N_3O_4$; during temperature around 140 °C with purification of 70%; FTIR results indicated 3429 cm^{-1} for OH hydroxyl group, 3139 cm^{-1} for C-H aromatic group stretching, 2939 cm^{-1}, 2859 cm^{-1} due to C-H groups, 1669 cm^{-1} for C=O carbonyl group, 1591, 1551, 1469 for C=N and C=C groups; As well as proton NMR in DMSO solvent beside TMS reference, indicated the chemical shifts as follows δ = 8.49 for HC=N imine, 7.71 HC=N pyrimidine ring , and 7.38-7.19 cm^{-1} for Ar-H , 6.39 cm^{-1} for HC=N pyrimidine ring. In addition, ^{13}C-NMR at (75 MHZ) exhibited δ =165.01, 149.72, 145.12, 129.75, 129.48, and 130.84 for those bonds, respectively.

3.1.3. "G3": Gemcitabine derived by 4-chlorobenzaldehyde

This compound was prepared through mentioned instruction by formula: $C_{16}H_{14}ClF_2N_3O_4$; during temperature around 170 °C with purification of 80%**;** FTIR results indicated 3425 cm^{-1} for OH hydroxyl group, 3119 cm^{-1} for C-H aromatic group stretching, 2945 cm^{-1}, 2832 cm^{-1} due to C-H groups, 1590, 1540, 1490 for C=N and C=C groups. As well as proton NMR in DMSO solvent beside TMS reference, indicated the chemical shifts as follows δ = 8.59 for HC=N imine, 7.69 for HC=N pyrimidine ring, and 7.29-7.19 cm^{-1} for Ar-H, 6.38 cm^{-1} HC=N pyrimidine ring. In addition, ^{13}C-NMR at (75 MHZ) exhibited δ =165.21, 151.72, 143.15, 132.70, 131.33, and 129.64 for those bonds, respectively.

3.1.4. "G4": Gemcitabine derived by N, N- di-methyl-benzaldehyde

This compound was prepared through mentioned instruction by formula:$C_{18}H_{20}F_2N_4O_4$ during temperature around 188 °C with purification of 80%**;** FTIR results indicated 3449 cm^{-1} for OH hydroxyl group, 3120 cm^{-1} for C-H aromatic group stretching, 2959 cm^{-1}, 2850 cm^{-1} due to C-H groups, 1669 for C=O stretching, 1589, 1580 for C=N and C=C groups. As well as proton NMR in DMSO solvent beside TMS reference, indicated the chemical shifts as follows δ = 8.39 for HC=N imine, 7.70 for HC=N pyrimidine ring, and 7.28-7.18 cm^{-1} for Ar-H, 6.39 cm^{-1} HC=N pyrimidine ring. In addition, ^{13}C-NMR at (75 MHz) exhibited δ =167.01, 154.89, 143.99, 139.98, 130.43, and 130.11 for those bonds, respectively.

3.1.5. "G5": Gemcitabine derived by 4-hydroxybenzaldehyde

This compound was prepared through mentioned instruction by formula: $C_{16}H_{15}F_2N_3O_5$; during temperature around 170 °C with purification of 69%**;** FTIR results indicated 3429 cm^{-1} for OH hydroxyl group, 3119 cm^{-1} for C-H aromatic group stretching , 2960 cm^{-1}, 2870 cm^{-1} due to C-H groups, 1580, 1540 for C=N and C=C groups. As well as proton NMR in DMSO solvent beside TMS reference, indicated the chemical shifts as follows δ = 8.38 for HC=N imine, 8.01 for HC=N pyrimidine ring, and 7.30-7.19 cm^{-1} for Ar-H, 5.80 cm^{-1} HC=N pyrimidine ring. In addition, ^{13}C-NMR at (75 MHZ) exhibited δ =165.31, 154.99, 152.98, 143.89, 130.99, and 130.01 for those bonds, respectively.

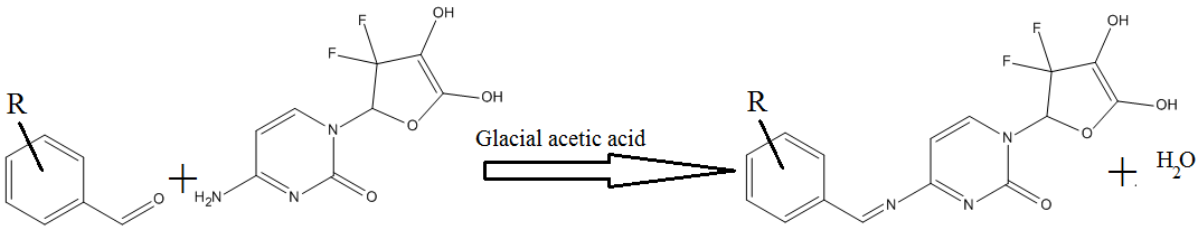

R=4-N,N-dimethyl ;4-Br ;4-Cl; 4-OH; 4-methyl

Figure 7. Schiff base derivatives of Gemcitabine.

Imine derivatives of compounds of gemcitabine have been prepared by reaction gemcitabine and several aromatic benzaldehydes. The chemical structures of all the end products were identified by some spectroscopic methods including ^{1}H-NMR, ^{13}C-NMR, FTIR, and elemental analysis. The ^{1}H-NMR spectrum of compounds exhibited lack of the amines' proton at δ=6.8 ppm in gemcitabine (Figure 8), but instead of that exhibited a new signal at 8.51, 8.49, 8.59, 8.39, and 8.01 for G1 to G5, ppm respectively for the protons of imine group N=CH

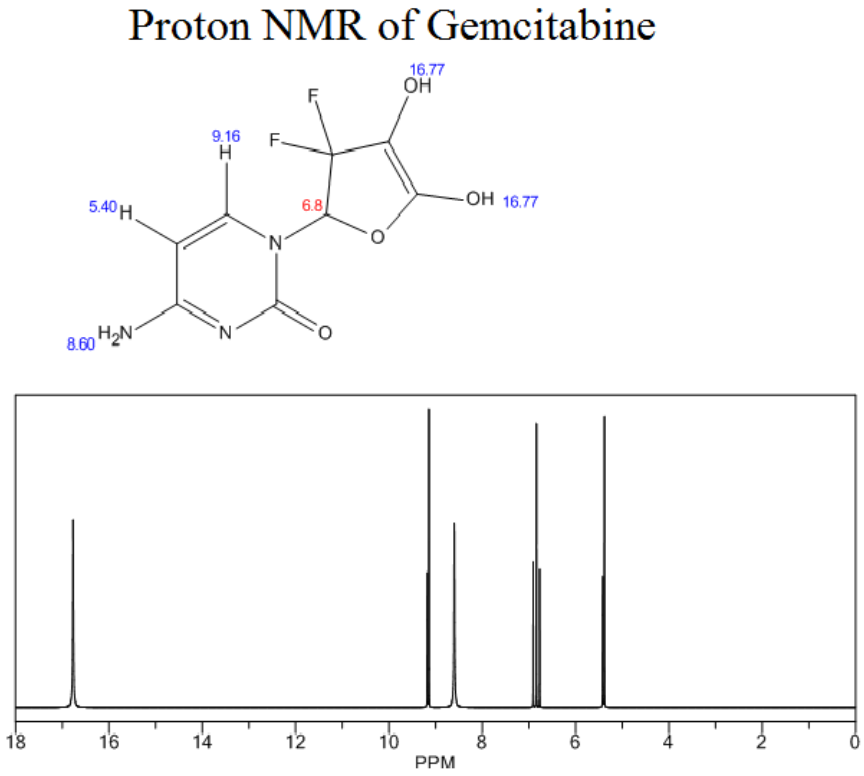

Figure 8. Proton NMR of pure Gemcitabine.

The ^{13}C-NMR spectrum of imine groups exhibited several new signals of the carbon imine group N=CH at 165.02 ppm, 165.01 ppm, 165.21 ppm, 167.01 ppm, and 165.31 ppm for G1 to G5, respectively these signals can be compared with ^{13}CNMR spectrum of pure Gemcitabine (Figure 9). On the other hand, the FT-IR spectra exhibited the stretching vibration of the imine group in complexes for G1-G5 and also two absorption bands of the asymmetric and symmetric stretching vibration of NH_2 group from gemcitabine disappeared after reaction of gemcitabine with several benzaldehydes (G1-G5) (Figure 9).

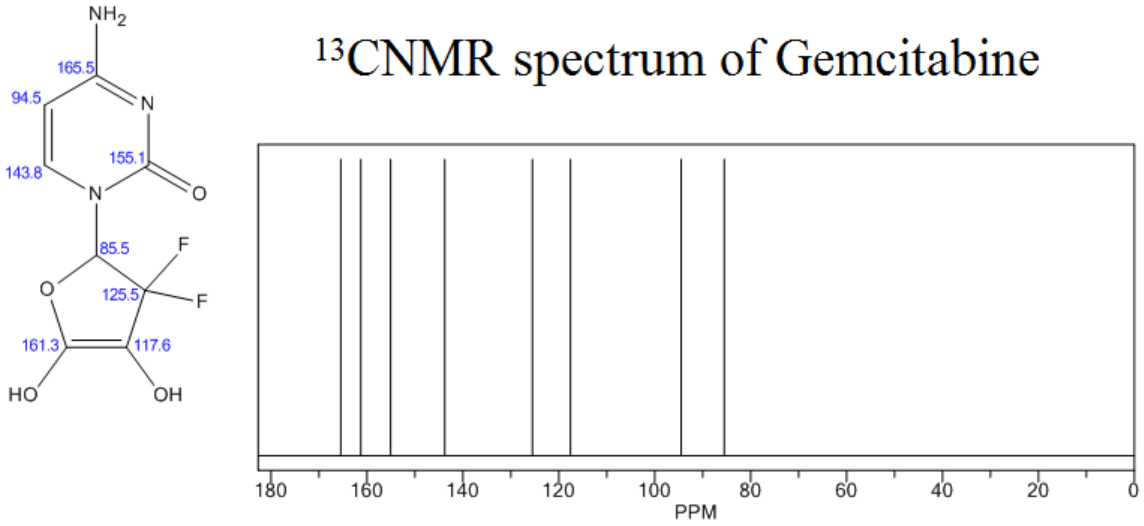

Figure 9. ^{13}C-NMR spectrum of pure Gemcitabine.

3.2. Poly (ethylene glycol) (PEG) spacer and linker for conjugate drugs

Poly (ethylene glycol) (PEG) is the most important polymer in delivering anticancer drugs clinically. PEGylation which means the covalent attachment of PEG to segment of peptides proteins drugs, is known to enhance the aqueous solubility of hydrophobic such drugs. This system increase circulation time and decreases nonspecific uptake, and achieve specific tumor target-ability through the enhanced permeability and retention effect. Currently various PEG-treatments has been developed, and several have received market approval. A vast amount of clinical experience has been gained which has helped to design PEG prodrug conjugates with improved therapeutic efficacy and reduced systemic toxicity. However, more efforts in designing PEG-based prodrug conjugates are anticipated. According to these properties we suggest a combination of Methotrexate with PEG spacer to link to the gemcitabine derivatives that can be used for any further testing for gynecological disease are shown in (Figure 10). Due to each of these structural properties, it can be predicted and then tested for various oncology cancers. These synthetic advances in PEG prodrug conjugation methodologies with varied bioactive components of clinical relevance could be synthesized for any approving by FDA-towards intended clinical applications, and formulations under clinical trials.

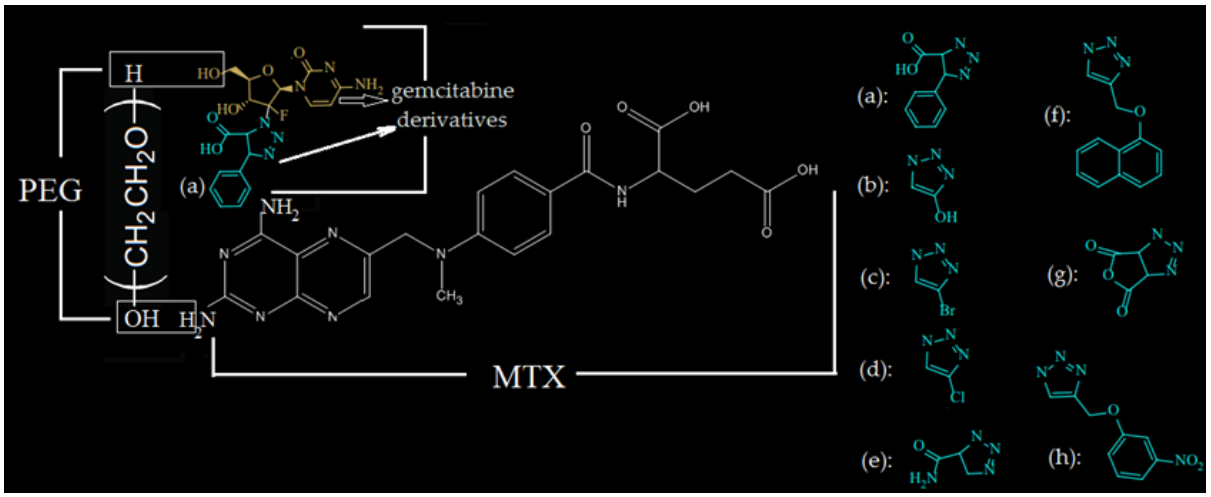

Figure 10. Methotrexate (MTX) with PEG spacer to link to the gemcitabine (GEM) derivatives.

3.3. Ligand and protein preparation

Chemical structures were drawn by ChemDraw (version 19.0.1.8, PerkinElmer) and then open into Chem3D Ultra (version 19.0.1.8, PerkinElmer). First optimization was accomplished using MM2 and MMFF9 force felids and modified in accurate form of three-dimensional geometries for precise structural analysis, and saved in Zmt format. Finally, through Gaussian 2016 ab-initio optimization was done in b3LYP/6-31g* level of theory. Two important gynecological disease proteins one for each cancer cell line (2Q79, 5J6R) was selected for molecular docking simulations. The docking efficiency was confirmed by re-docking the sample ligands of 4ZXT and 7LXL, according to the resulting RMSD at 1.79 Å and 1.20 Å, respectively.

4. RESULTS AND DISCUSSION

4.1. Proteins based on relevance to gynecological cancers

The goal for choosing of the proteins were based on relevance to gynecological disease of several cancers using the Protein Data Bank (PDB), and the mechanism of each system were considered according to critical oncogenic signaling pathways. 2Q79 is related to the crystal structure of single chain E2C from HPV16 [24, 25]. The E2 DNA-binding is related to the cervical cancer-associated strain human papillomavirus type 16 (HPV-16) in gynecological disease. The papillomavirus E2 proteins regulate transcription from all viral promoters, which belong to a group of viral proteins in dimeric β-barrels form that apply surface α-helices during DNA intercalation. Although all E2 proteins are identical in palindromic DNA sequence, proteins of various viral strains differ in their potential to discriminate among their specific DNA-binding sites. The protein data x-ray indicates that though the folding of HPV-16 E2 DNA-binding domain resembles replant to the viral strain papillomavirus type 1, the accurate configuration for the recognition helices is completely different, due to the charge distribution on the DNA-binding area and less electropositive surface for E2. Therefore, HPV-16 E2 is thus less able to utilize charge neutralization of the phosphate groups on DNA to induce bending which causes reducing affinity between HPV-16 E2 and flexible DNA target sequences, in other hands enhanced affinity towards A-tract-containing, pre-bent sequences (Figure 11-a).

5J6R is related to the crystal structure of human papillomavirus type 59 L1 (Figure 11-b). This virus belongs to the Papillomaviridae category that consists of 199 different genotypes containing different tropism and pathogenesis. Generally, they categorized as low and high risk dangerous based on their ability to induce cancer. Carcinogenic HPV types include HPV16, HPV18, HPV31, HPV33, HPV35, HPV39, HPV45, HPV52, HPV56, HPV51, HPV58,

and HPV59. Two other types which known as HPV68 and HPV66, although often exhibits medium-risk, have a dangerous capacity to induce cancer. Although most of these viruses affected to various cancers, oncogenic types have been linked to cervix, anal, vulva, vagina, penile. Worldwide, HPV infection still causes up to 4.5% (630 000 cases) of all new cancer cases worldwide (8.6% in females; 0.9% in males), representing 29.5% of all infection-related cancers.

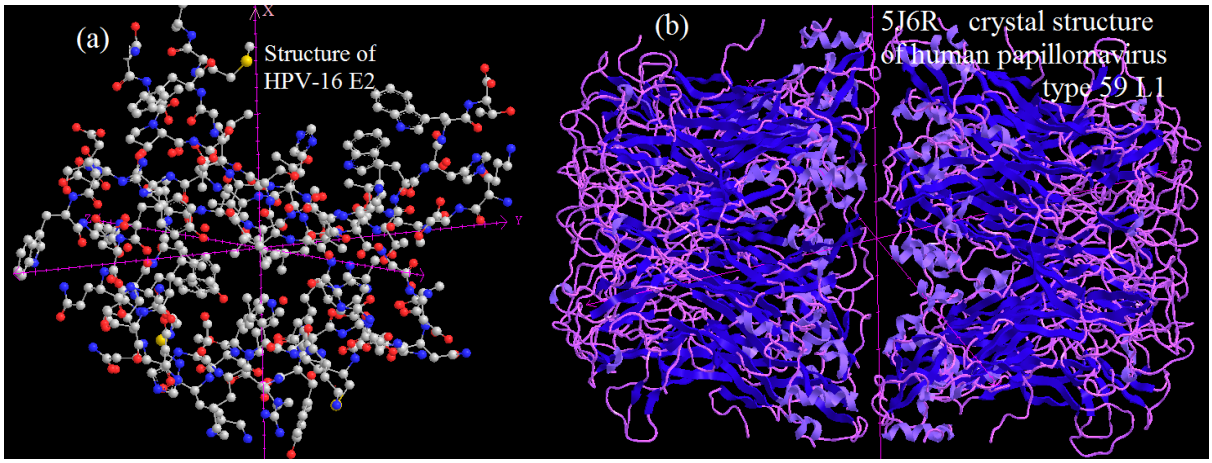

Figure 11. (a) Optimized stricture of HPV-16 E2 with charm software; (b) human papillomavirus type 59 L1 from protein data bank.

Prophylactic HPV vaccines have been progressively introduced worldwide since 2006. Large phase III randomized clinical trials and post-licensure studies and trials have proven high efficacy, effectiveness, and safety records in the prevention of vaccine-type HPV infection and cancer precursor lesions (cervical intraepithelial neoplasia. Although currently, three HPV vaccines are commercially available that include of virus-like particles (VLPs) of HPVs 16/18, the four valent and nine valent vaccines also prepared by VLPs from HPVs 6/11. The bivalent type has exhibited a suitable index against whole of gynecological cancers. This cross-protection has been recently corroborated in observational studies from Scotland. World public health reported, which these vaccines offer comparable immunogenicity, efficacy, and effectiveness for the prevention of cervical cancer, mainly caused by HPV16 and HPV18. In accordance with the genotype attribution to different cancer sites, the existing vaccines could prevent up to 90% of HPV-associated cancers and related pre-neoplastic lesions. Here by we studied 7 central signals with frequent tumor genome alterations, with keyword oncology discovered in these pathways in previous GOA work, and focused on various pathways that are potential drivers of cancer. The routs analyzed are: cell cycle, gynecologic signaling, Myc 4) oxidative stress response / NRF2, PI-3-Kinase signaling, receptor-tyrosine kinase (RTK) / RAS / MAP-Kinase signaling, TGFβ signaling, P53, and β-catenin / WNT were signaling. Alterations in DNA repair pathways, epigenetic modifiers, splicing, and other cellular mechanisms have not been implicated in cancer because these mechanisms mainly underlie genomic instability compared with specific proliferative potential. We began by reviewing the complete set of tumor-disease pathway mappings from the GOA compendium between 2010 and 2023, each of which included pathway genes genetically altered in tumor types. These route diagrams are publicly available as predefined network templates on the www (Figure 12). Considering the association of pathway members across multiple GOA studies, we generated a consolidated list of candidate member genes for each of the 7 pathways. It was then organized based on the updated literature.

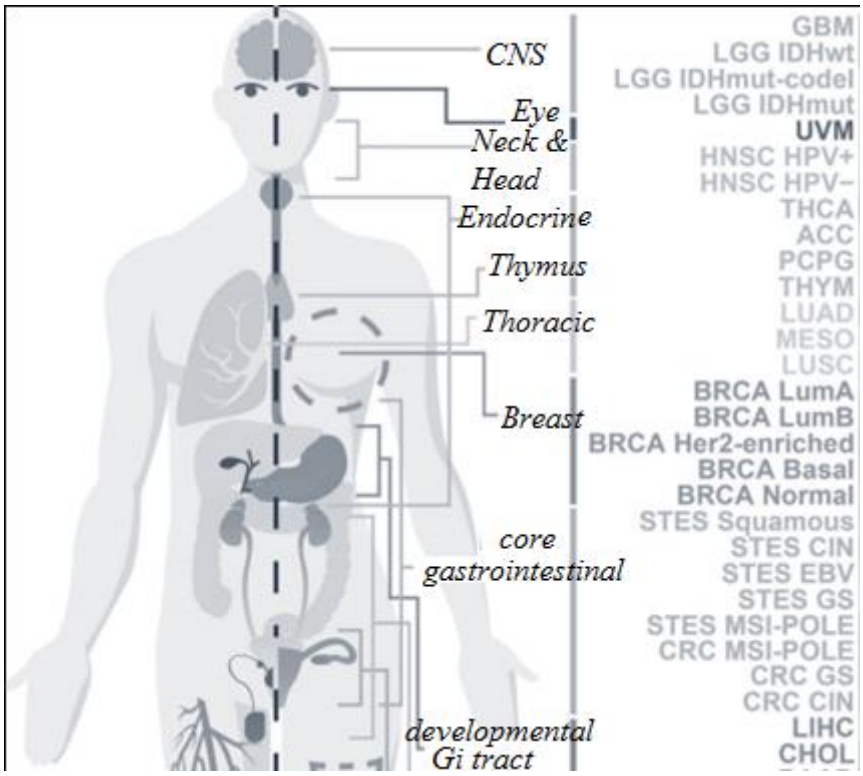

Figure 12. Changed samples in pathway of gynecologic oncology types and tumor subtype.

4.2. Docking simulation

We simulated our model based on our previous works [26-32]. Favorable interactions with the major active site residues were also visualized by binding mode inspection. The computational technique MVD was used for 6 compounds against several different cancer cell lines including 2Q79, 5J6R, and and6BIM from protein data bank. The threshold for docking scores was established by comparing the docking scores of the test compounds with the reference drug gemcitabine and G1 up to G5 compounds. All five complexes exhibited more negative amounts than gemcitabine and g5 was considered to have better binding affinities compared with others (Figure 13). The main target was to determine the stable structure including minimum potential energy, where MVD operates by replacing cavities on the protein active sites, generating poses, and selecting the best pose based on the MolDock score (Figures 13-15).

iGEMDOCK

Protein Ligand Docking/Screening | Docked Poses/Post-Screening Analysis | About

1. Prepare Screening Data

Load | Binding Site | esktop/2Q79.pdb | Docked Poses

Generate | Interaction Profile | Interaction Analysis

Output

C:/Users/sahar/Desktop/iGEMDOCKv2.1/output/ | Set Output Path

Save | Summary table | Text | Excel

Select | All | / | None | Compounds | Display | Sort | Compound | Clean Table

	Compound	Energy	VDW	HBond	Elec
Doc -1	2Q79-G1	-64.41	-42.41	-22.31	-17.43
Doc -2	2Q79-G 2	-62.33	-41.45	-21.73	-17.11
Doc -3	2Q79-G 3	-60.45	-40.55	-20.85	-16.87
Doc -4	2Q79-G 4	-67.39	-46.93	-23.61	-17.93
Doc - 5	2Q79-G 5	-70.66	-49.66	-25.44	-20.47
Doc - 6	2Q79-Gemcitabine	-55.88	-39.98	-19.45	-15.67

Figure 13. Docking simulation data for G1 to G5 including pure Gemcitabine.

Using Molegro Virtual Docker, several possible binding sites were identified in the crystal structure (PDB ID: 2Q79). The MVD workspace was then exported to Discovery Studio, providing a more visually intuitive representation of interactions between protein and ligand, elucidating their type, category, and bond distances. Additionally, all 2Q79-binding compounds formed stable hydrogen bonds and hydrophobic contacts with essential residues binding pocket, including 2Q79, 5J6R, and 6BIM (interaction details in Figure 13). Gemcitabine has a demonstrated inhibitory effect on the reduction in ERK2 phosphorylation, in various types of cancer cells.

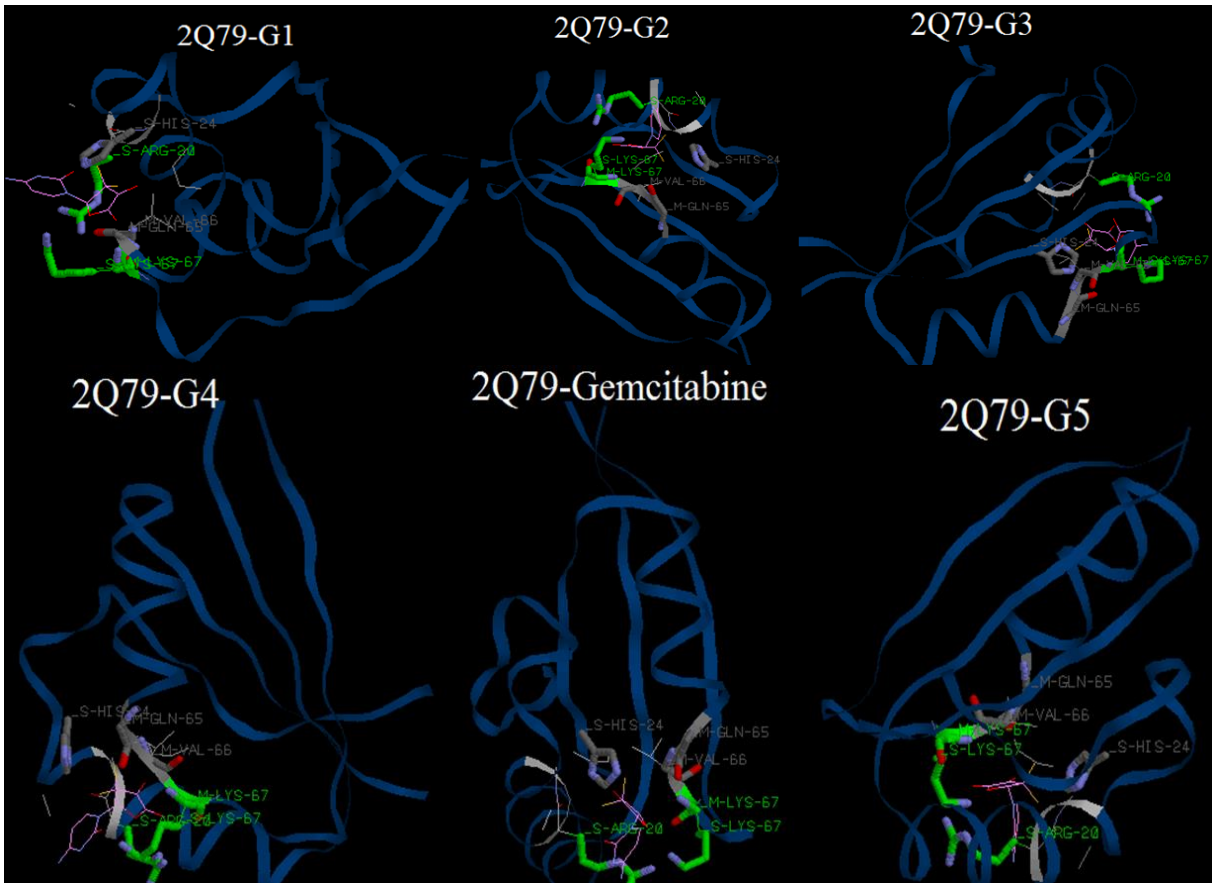

Figure 14. Favorable interactions with the major active site residues were also visualized by binding mode inspection for 6 positions.

Five protein–ligand complexes emerged as leads based on their scores. Investigating, which 2Q79-G5 gave the highest Mol-Dock score energies of −77.66 compared with 2Q79-Gemcitabine which is -55.88. The rest were also over 2Q79-Gemcitabine with sequence as: 2Q79-Gemcitabine <2Q79-G3 <2Q79-G2 <2Q79-G1 <2Q79-G4 <2Q79-G-5. Remarkably, 2Q79-G-5 demonstrated a total of 8 interactions, including hydrogen bonds and carbon–hydrogen bonds with amino acids H-S-Arg20, H-M LYS67, H-S LYS67, V-S-Arg20, V-S-His24, V-M-Gln65, V-M-Val66, and V-S-Lys67 (Figure 15).

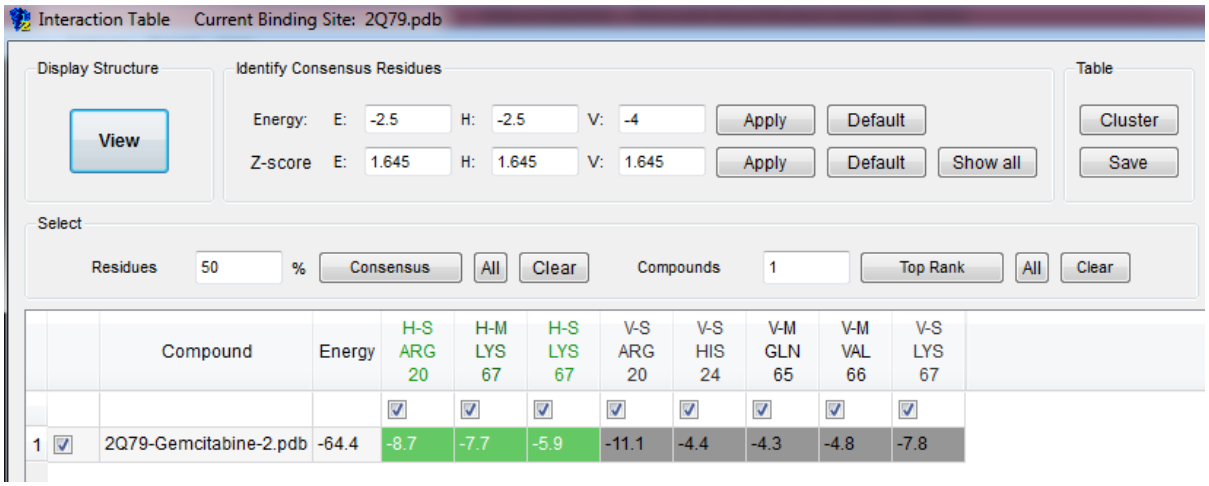

Figure 15. 2Q79-G-5 demonstrated a total of 8 interactions, including hydrogen bonds and carbon–hydrogen bonds with amino acids.

Some of them had shown a total of 6 interactions, including hydrogen bonds, carbon–hydrogen bonds, π–sigma, π–sulfur, π–lone pair, π–π T-shaped, and π–alkyl interactions with amino acids L.

5. CONCLUSION

Oncology genetic counseling has become more common for women with significant risks for certain genetic diseases, especially for women with concerns about potentially fatal conditions such as Tay-Sachs, lifelong health risks from sickle cell anemia, or BRCA gene mutations, which increases the risk of breast cancer. If obstetrics and gynecology patients could receive personalized risk assessments for these conditions without considering physician services, wouldn't they be able to make smarter choices about their health or family planning. For example, insurers and health care providers who increasingly bet their financial resources on patient outcomes may be less willing to treat or cover patients of Gynecologic oncology they perceive to be at higher-than-average risk of developing a disease. And physicians already overwhelmed with patient-generated health data, reports and reminders from other providers, and the daily burden of electronic health record use, population health management, and intense financial pressures may not know what to do with this information.

CONFLICTS OF INTEREST

The authors declare that there is no conflict of interest.

REFERENCES

1. K. Brown, A. Weymouth-Wilson & B. Linclau. A linear synthesis of gemcitabine. *Carbohydrate Research*, **406**, 71–75 (2015). https://doi.org/10.1016/j.carres.2015.01.001
2. K.K.Y. Cham, J.H. Baker, K.S. Takhar, J.A. Flexman, M.Q. Wong, D.A. Owen, *et al.* Metronomic gemcitabine suppresses tumour growth, improves perfusion, and reduces hypoxia in human pancreatic ductal adenocarcinoma. *British Journal of Cancer*, **103**, 52–60 (2010). https://doi.org/10.1038/sj.bjc.6605727
3. G. Bocci, R. Danesi, G. Marangoni, A. Fioravanti, U. Boggi, I. Esposito, *et al.* Antiangiogenic versus cytotoxic therapeutic approaches to human pancreas cancer: an experimental study with a vascular

endothelial growth factor receptor-2 tyrosine kinase inhibitor and gemcitabine. *European Journal of Pharmacology*, **498**(1-3), 9–18 (2004). https://doi.org/10.1016/j.ejphar.2004.07.062

4. S.A. Veltkamp, J.H. Beijnen & J.H.M. Schellens. Prolonged versus standard gemcitabine infusion: translation of molecular pharmacology to new treatment strategy. *The Oncologist*, **13**(3), 261–276 (2008). https://doi.org/10.1634/theoncologist.2007-0215
5. L.J. Scott & C.M. Spencer. Miglitol: a review of its therapeutics potential in type 2 diabetes mellitus. *Drugs*, **59**(3), 521–549 (2000). https://doi.org/10.2165/00003495-200059030-00012
6. B. Mayur, S. Sandesh, S. Shruti & S. Sung-Yum. Antioxidant and α-glucosidase inhibitory properties of *Carpesium abrotanoides*. *Journal of Medicinal Plants Research*, **4**(15), 1547–1553 (2010). URL: https://academicjournals.org/article/article 1380703440_ Mayur %20et%20al%20PDF.pdf
7. M. Das, R. Jaine, A.K. Agrawal, K. Thanki & S. Jain. Macromolecular bipill of gemcitabine and methotrexate facilitates tumor-specific dual drug therapy with higher benefit-to-risk ratio. *Bioconjugate Chemistry*, **25**(3), 501–509 (2014). https://doi.org/10.1021/bc400477q
8. K. Brown, A. Weymouth-Wilson & B. Linclau. A linear synthesis of gemcitabine. *Carbohydrate Research*, **406**, 71–75 (2015). https://doi.org/10.1016/j.carres.2015.01.001
9. S. Yang, D. Luo, N. Li, C. Li, S. Tang & Z. Huang. New mechanism of gemcitabine and its phosphates: DNA polymerization disruption via 3′–5′ exonuclease inhibition. *Biochemistry*, **59**(45), 4344–4352 (2020). https://doi.org/10.1021/acs.biochem.0c00543
10. A. El-Laghdach, M.I. Matheu, S. Castillón, C. Bliard, A. Olesker & G. Lukacs. A new and extremely fast synthesis of 2-deoxy-2,2-difluoro-d-arabino-hexose (2-deoxy-2,2-difluoro-d-glucose). *Carbohydrate Research*, **233**, C1–C3 (1992). https://doi.org/10.1016/S0008-6215(00)90944-3
11. A. Rouf, M.A. Aga, B.Kumar, S.Taneja, (R)-2,3-Cyclohexylideneglyceraldehyde, a Chiral Pool Synthon for the Synthesis of 2-Azido-1,3-diols, *Helvetica Chimica Acta*, **98**(6) (2015). DOI:10.1002/hlca.201400344
12. J.A. Weigel. A new method for the synthesis of α,α-difluoro-β-hydroxy esters through the enolization of s-tert-butyl difluoroethanethioate. *The Journal of Organic Chemistry*, **62**(18), 6108–6109 (1997). https://doi.org/10.1021/jo9711596
13. Y. Matsumura, H. Fujii, T. Nakayama, Y. Morizawa & A.J. Yasuda. Titanium-promoted highly stereoselective synthesis of α,α-difluoro-β,γ-dihydroxyester. Simple route to 2-deoxy-2,2-difluororibose. *Journal of Fluorine Chemistry*, **57**(1-3), 203–207 (1992). https://doi.org/10.1016/s0022-1139(00)82832-8
14. M. Monajjemi, M.H. Razavian, F. Mollaamin, F. Naderi & B. Honarparvar. A theoretical thermochemical study of solute-solvent dielectric effects in the displacement of codon-anticodon base pairs. *Russian Journal of Physical Chemistry A,* **82**(13), 2277–2285 (2008). https://doi.org/10.1134/s0036024408130207
15. F. Mollaamin, S. Shahriari & M. Monajjemi. Therapeutic role of medicinal plants against viral diseases focusing on COVID-19: Application of computational chemistry towards drug design. *Revista Colombiana de Ciencias Químico-Farmacéuticas*, **53**(1), 19–43 (2024). https://doi.org/10.15446/rcciquifa.v53n1.112978
16. F. Mollaamin & M. Monajjemi. Drug delivery using doping of boron nitride nanosensor towards releasing chloroquine drug in the cells: A promising method for overcoming viral disease. *Revista Colombiana de Ciencias Químico-Farmacéuticas*, **53**(2), 430–454 (2024). https://doi.org/10.15446/rcciquifa.v53n2.114450
17. M. Monajjemi, H. Aghaie & F. Naderi. Thermodynamic study of interaction of TSPP, CoTsPc, and FeTsPc with calf thymus DNA. *Biochemistry Moscow*, **72**(6), 652–657 (2007). https://doi.org/10.1134/s0006297907060089
18. F. Mollaamin & M. Monajjemi. Molecular modelling framework of metal-organic clusters for conserving surfaces: Langmuir sorption through the TD-DFT/ONIOM approach. *Molecular Simulation*, **49**(4), 365–376 (2023). https://doi.org/10.1080/08927022.2022.2159996
19. F. Mollaamin & M. Monajjemi. Transition metal (X = Mn, Fe, Co, Ni, Cu, Zn)-doped graphene as gas sensor for CO_2 and NO_2 detection: a molecular modeling framework by DFT perspective. *Journal of Molecular Modeling*, **29**(4), 119 (2023). https://doi.org/10.1007/s00894-023-05526-3

20. M. Monajjemi, F. Naderi, F. Mollaamin & M. Khaleghian. Drug design outlook by calculation of second virial coefficient as a nano study. *Journal of the Mexican Chemical Society*, **56**(2), 207–211 (2012). https://doi.org/10.29356/jmcs.v56i2.323
21. M. Monajjem, N. Karachi & F. Mollaamin. The investigation of sequence-dependent interaction of messenger RNA binding to carbon nanotube. *Fullerenes, Nanotubes and Carbon Nanostructures*, **22**(7), 643–662 (2014). https://doi.org/10.1080/1536383x.2012.717557
22. M. Monajjemi. Quantum investigation of non-bonded interaction between the $B_{15}N_{15}$ ring, and BH_2NBH_2 (radical, cation, anion) systems: A nano molecularmotor. *Structural Chemistry*, **23**(2), 551–580 (2012). https://doi.org/10.1007/s11224-011-9895-8
23. M. Monajjemi & J.E. Boggs. A new generation of BnNn rings as a supplement to boron nitride tubes and cages. *Journal of Physical Chemistry A*, **117**(7), 1670–1684 (2013). https://doi.org/10.1021/jp312073q
24. I. Zehbe, E. Wilander, H. Delius & M. Tommasino. Human papillomavirus 16 E6 variants are more prevalent in invasive cervical carcinoma than the prototype. *Cancer Research*, **58**(4), 829–833 (1998). URL: https://pubmed.ncbi.nlm.nih.gov/9485042/
25. L.F.Xi, G.W. Demers, L.A. Koutsky, N.B. Kiviat, J. Kuypers, D.H. Watts, K.K. Holmes & D.A. Galloway. Analysis of human papillomavirus type 16 variants indicates establishment of persistent infection. *The Journal of Infectious Diseases*, **172**(3), 747–755 (1995). https://doi.org/10.1093/infdis/172.3.747
26. F. Mollaamin, J. Najafpour, S. Ghadami, A.R. Ilkhani, M. Akrami & M. Monajjemi. The electromagnetic feature of $B_{15}N_{15}Hx$ (x = 0, 4, 8, 12, 16, and 20) nano, rings: Quantum theory of atoms in molecules/NMR approach. *Journal of Computational and Theoretical Nanoscience*, **11**(5), 1290–1298 (2014). https://doi.org/10.1166/jctn.2014.3495
27. M. Monajjemi & F. Mollaamin. Intermolecular simulation of nanobiological structures in point of potential energy and second virial coefficient. *Journal of Computational and Theoretical Nanoscience*, **9**(12), 2208–2214 (2012). https://doi.org/10.1166/jctn.2012.2640
28. F. Mollaamin & M. Monajjemi. Electric and magnetic evaluation of aluminum–magnesium nanoalloy decorated with germanium through heterocyclic carbenes adsorption: A density functional theory study. *Russian Journal of Physical Chemistry B*, **17**(3), 658–672 (2003). https://doi.org/10.1134/s1990793123030223
29. M. Monajjemi, S. Ketabi, M.H. Zadeh & A. Amiri. Simulation of DNA bases in water: Comparison of the Monte Carlo algorithm with molecular mechanics force fields. *Biochemistry Moscow*, **71**(Suppl. 1), S1–S8 (2006). https://doi.org/10.1134/s0006297906130013
30. F. Mollaamin & M. Monajjemi. Graphene-based resistant sensor decorated with Mn, Co, Cu for nitric oxide detection: Langmuir adsorption & DFT method. *Sensor Review*, **43**(4), 266–279 (2023). https://doi.org/10.1108/SR-03-2023-0040
31. M. Monajjemi, B. Honarparvar, S.M. Nasseri & M. Khaleghian. NQR and NMR study of hydrogen bonding interactions in anhydrous and monohydrated guanine cluster model: A computational study. *Journal of Structural Chemistry*, **50**(1), 67–77 (2009). https://doi.org/10.1007/s10947-009-0009-z
32. B. Khalili-Hadad, F. Mollaamin & M. Monajjemi. Biophysical chemistry of macrocycles for drug delivery: A theoretical study. *Russian Chemical Bulletin*, **60**(2), 238–241 (2011). https://doi.org/10.1007/s11172-011-0039-5

HOW TO CITE THIS ARTICLE

M. Monajjemi, F. Mollaamin, A. Ghadami, R. Souri, Z. Aghakouchaki, M. Aghaei, Z. Solati & Y. Shahverdy. Cancer drug therapy by Gemcitabine derivatives with PEG linker for gynecological disease, beside speech therapy in implementation of biomedical caring of post-operative. *Rev. Colomb. Cienc. Quim. Farm.*, **55**(1), 151–166 (2026). https://doi.org/10.15446/rcciquifa.v55n1.125080